Identification of the heat flux generated by friction in an aircraft braking system

Jean-Gabriel Bauzin, Nicolas Keruzore, Najib Laraqi, Arnaud Gapin, Jean-Frédéric Diebold

IDENTIFICATION OF THE HEAT FLUX GENERATED BY FRICTION IN AN AIRCRAFT BRAKING SYSTEM

Jean-Gabriel BAUZIN [a,*1], ***Nicolas KERUZORE*** [a,b], ***Najib LARAQI*** [a], ***Arnaud GAPIN*** [b], ***Jean-Frédéric DIEBOLD*** [b],

[a] Université Paris Nanterre, Laboratoire Thermique Interfaces Environnement (LTIE), EA 4415, 50 rue de Sèvres, 92410 Ville d'Avray – France
[b] SAFRAN LANDING SYSTEMS, Methods & Tools Engineer – Thermal simulation, Wheels & Brakes Division, Site Jean-Paul Béchat, Inovel Parc Sud, 7 rue Général Valérie André, 78140 Vélizy-Villacoublay - France

Abstract
In this paper, we present an estimation of the heat flux generated by friction under real aircraft braking conditions using an inverse method. The estimation is performed considering an assumption of 1D transient model and multiple interfaces. This model takes into account a non-perfect description of the thermal contact. Then, an identification of the generated heat flux by friction in the different interfaces from experimental data is performed using a linear temporal evolution parameterization of this parameter. The reconstruction of the thermal field from identified generated heat fluxes provides some very low residues. The comparison between the thermal energy identified by the inverse method and mechanical energy absorbed on the test bench validates the results.

Keywords: *Estimation of thermal contact parameters, aircraft braking, inverse methods.*

1. Introduction

Modern civil planes are prone to take-off and land several times a day. Companies' willingness to reduce turnaround time (TAT) and to reduce the weight of the brake, leads to very high loads and temperature in carbon disks. Although temperature estimation or measurement seems natural, friction heat flux at disk contacts is not well-defined. Besides, 3D model robustness and accuracy are non-optimal, since the causes of heat fields are not perfectly determined. The aim of this study is to characterize in-landing boundary conditions at carbon disk surfaces from thermal measurements on an experimental device. Among all the type of inverse heat conduction problems (IHCP), we are interested here in the identification of an unknown heat flux boundary condition. Inverse heat conduction problems are highly ill-posed, to the extent that any small input modification results in a pronounced modification of the solution. Many investigations have presented several methods in improving the stability of IHCP [1]–[7]. Although many works deal with experimental and numerical analysis of direct heat transfer problem in the automotive or rail brake disc [8]–[14], very few studies concerning IHCP in disc brakes have been published. Furthermore, most studies often use numerical simulations as data [15]. Ghadimi [16] presents an inverse algorithm based on the Artificial Neural Networks and the Sequential Function in order to estimate the heat flux absorbed by the locomotive brake disc. However, all these references present braking systems comprising only one disc. Fittingly, aircraft braking systems are composed of several discs in friction with multiple interfaces. Few references [17]–[21] deal with this configuration and all

[*]Corresponding author ; e-mail : jbauzin@parisnanterre.fr

of them develop Finite Element models. However, none specify the generated heat fluxes to be considered in these numerical models in order to determine the resulting temperature fields. In this study, we aim to identify these generated heat fluxes from experimental data, using one dimensional IHCP method. In order to solve the inverse problem, a simple direct model has to be developed. A Finite Difference Method (FDM) has been chosen to solve the direct problem.

Different regularization techniques can be used to stabilize the IHCP procedure as truncation or penalization [22], [23]. In order to identify the evolution of parameters, the estimation could be based on the function specification method using future time step [2]. Finally, for the problem of identifying the evolution of the heat flux generated by friction in an aircraft braking system, the parameterization of this evolution is used in the IHCP [24]–[26].

2. Brake thermal direct model

2.1 Presentation

For this study, the brake core is composed of nine carbon discs, including five stators and four rotors. The wheel and brake assembly is presented in figure 1. We propose to develop a simple thermal 1D model on the braking period, while the wheel is in rotation. During this period, we can consider that only the discs are subject to high temperature gradients. After this phase, which lasts a few seconds, the heat will be transferred to the other part of the braking system (the wheel, torque tube, piston housing...). The short scale of time allows us to consider brake surrounding temperatures, close to initial conditions.

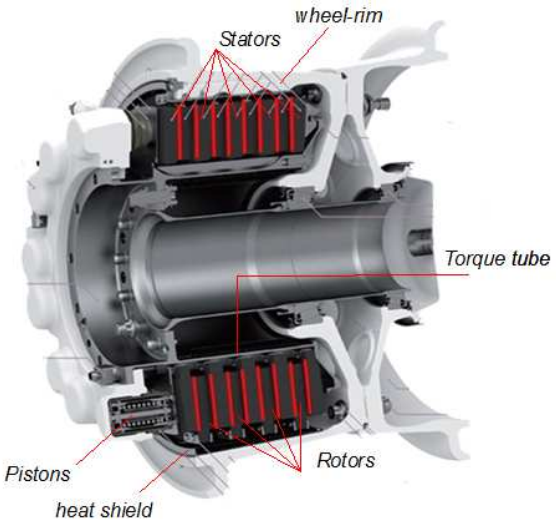

Figure 1. Studied aircraft braking system (see also figure 2)

During this time scale, a heat flux is generated by friction on the sliding contact surfaces between rotors and stators. Spatial and temporal heat flux distribution will condition the heat gradient within the brake system, and that is why its characterization is crucial. Currently, hypotheses based on brake mechanical behavior and efficiency are made but they have never been verified experimentally.

2.2 System modeling

At each interface between stators and rotors, the thermal contact is supposed to be non-perfect. Bardon [27] proposed an expression to describe the interfacial heat exchange. This approach introduces two contact parameters in addition to the generated heat flux: the sliding thermal contact resistance and the intrinsic heat partition coefficient. Both parameters are dependent upon the thermal constriction resistances. An equivalent expression has been proposed by Tseng [28] to study heat transfer for rolling systems. During the braking, heat propagation is supposed to be unidirectional in the entire system, following the transverse direction to the discs as is shown in figure 2. k^{th} rotor is noted as R_k, k^{th} stator as S_k, and the k^{th} sliding interface as I_k.

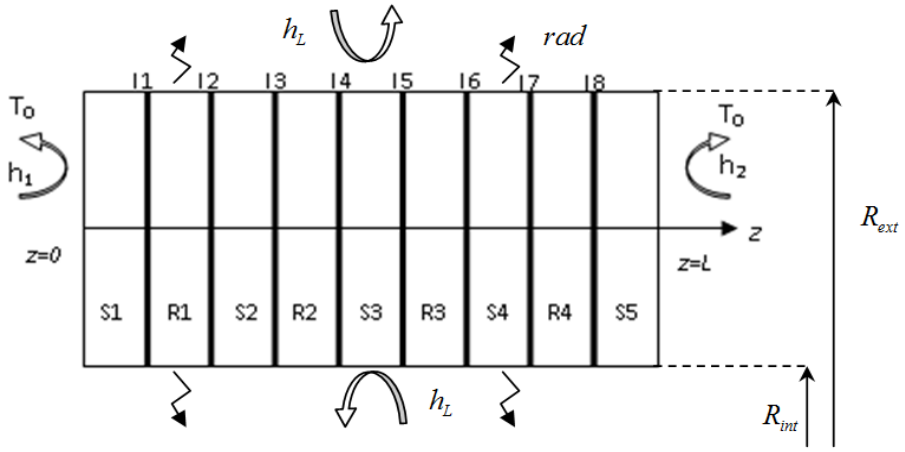

Figure 2. Representation of the studied 1D system

Carbon discs can then be considered as simple successive rings, with R_{ext} as their external radius, R_{int} as their internal radius, and with a non-perfect thermal contact model between each disk. At first, boundary conditions are set with Fourier conditions at left and right extreme boundaries. The heat equation is established in eq. (1) for our one-dimensional problem in *z* direction. Moussa *et al.* [7] used a similar approach in their study of the heat transfer at the grinding interface between a glass plate and a sintered diamond wheel.

$$\begin{cases} \dfrac{1}{a}\dfrac{\partial T}{\partial t}=\dfrac{\partial^2 T}{\partial z^2}-\dfrac{h_L}{\lambda}C_0\left(T(z,t)-T_0\right)-\dfrac{\sigma\varepsilon_L}{\lambda}C_1\left(T^4(z,t)-T_S{}^4\right)-\dfrac{\sigma\varepsilon_L}{\lambda}C_2\left(T^4(z,t)-T_T{}^4\right) \\ \lambda\dfrac{\partial T}{\partial z}\Big|_{z=0}=h_1\left(T-T_0\right),\ -\lambda\dfrac{\partial T}{\partial z}\Big|_{z=L}=h_2\left(T-T_0\right),\ T\left(z,t=0\right)=T_0 \\ \varphi_{l_k}(t)=\alpha_k\ \varphi_{gk}(t)+\dfrac{T_{cl_k}(t)-T_{cr_k}(t)}{R_{TSC_k}},\quad \varphi_{gk}=\varphi_{l_k}(t)+\varphi_{r_k}(t)\quad \text{on each interface } I_k \\ \text{with } C_0=\dfrac{2}{R_{ext}-R_{\text{int}}}, C_1=\dfrac{2R_{ext}}{\left(R_{ext}-R_{\text{int}}\right)^2}, C_2=\dfrac{2R_{\text{int}}}{\left(R_{ext}-R_{\text{int}}\right)^2} \end{cases} \tag{1}$$

Where $\varphi_{l_k}(t)$ and $\varphi_{r_k}(t)$ are the heat flux entering the left and the right-sided disc, respectively, R_{TSC_k} is the thermal contact resistance, $\varphi_{gk}(t)$ the generated heat flux, $T_{cl_k}(t)$ and $T_{cr_k}(t)$, respectively, are the contact temperatures on the left and right at the interface *k*

between a rotor and a stator at the time *t*. Because the frictional materials are identical, the local heat partition coefficient α_k is assumed to be equal to 0.5 for each interface according references [27], [28]. Time evolution of the generated heat flux $\varphi_k(t)$ will be discussed in part 2.3. Lateral losses by convection on the sides of the discs are taken into account with the ambient temperature, which is supposed to be constant. Lateral losses by radiation are calculated with the heat shield temperature T_S (on the external radius), and with the torque tube temperature T_T (on the internal radius). During the braking period, there is just a small variation of these surrounding temperatures. Therefore, we make the assumption that they remain constants for the radiation model. A parametric study is conducted in part 4 to analyze the effect of h_L and ε_L. We show that the convective and radiative heat losses (regardless of h_L and ε_L physical values) are negligible comparatively to the generated heat flux. These losses are less than 3% of the friction energy.

2.3. Parameterization of the problem

The different thermal contact parameters are: $\varphi_k(t)$ and R_{TSC_k}, α_k . The local heat partition coefficient is supposed to be equal to 0.5 (carbon/carbon sliding contact). In the aircraft braking system case, where the heat generated heat flux is important [29], the impact of the contact resistance on the temperature is insignificant. It will be difficult or impossible to identify this parameter [29], [30]. Therefore, the value of the sliding contact resistance will be imposed on $R_{TSC} = 10^{-4} m^2 KW^{-1}$. The impact on the identification procedure of this assumption will be insignificant on the other parameters, under 2% if $R_{TSC} <= 10^{-3} m^2 KW^{-1}$.

We propose to estimate a linear heat flux between step times. We use a generated heat flux parameterization with a hat function basis such as shown below in figure 3 [26]. The parameterization is an efficient regularization process for the inverse problem [25].

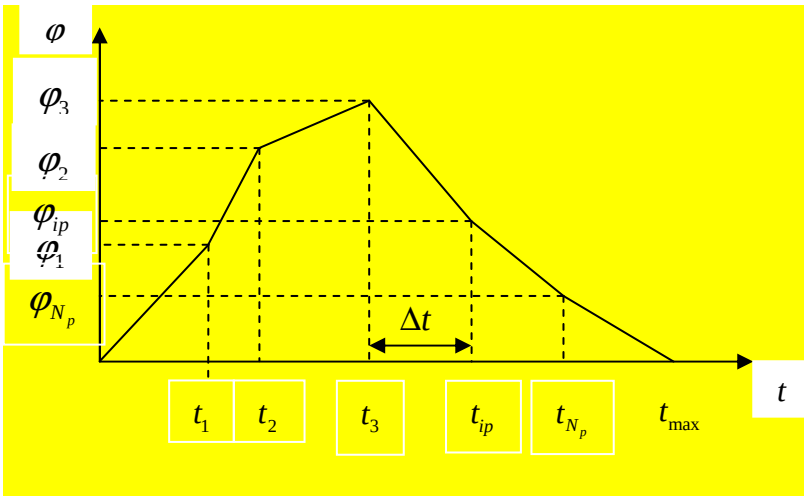

Figure 3. Heat flux function parameterization for each sliding interface

The choice of the time increment $\Delta t = t_{ip} - t_{ip-1}$ is based on the supposed variation form of the generated heat flux study. Indeed, if Δt is too small, it will be difficult to identify φ_{ip}. In fact, the heat flux must have sufficiently varied over a time increment in order to identify the

different function values. We note φ_{ip}^{k} as the different heat flux φ_{ip} at the interface *k*. $t_{\max}$ corresponds to the stop of the wheel.

2.4 Identification procedure

The different φ_{ip} have to be identified. The time vector is imposed and is chosen from the assumed rate of heat generated flux change during the braking period. The time increment will be less in the first braking period instants. Then, the parameter vector β to be identified is composed of the different φ_{ip}^{k} for each sliding interfaces $\beta = \left[\varphi_1^1 \; \varphi_2^1 \cdots \varphi_{ip}^k \cdots \varphi_{N_p}^8 \right]^T$. The vector estimation is performed by minimizing the square of the difference between measured data and calculated temperatures by the direct problem [4], [31], [32]. The functional of the least-square method is given by equation 2,

$$J(\beta) = \sum_{i=1}^{i=N} \sum_{j=1}^{j=M} \left(T_j^i - \tilde{T}^i{}_j \right)^2 \tag{2}$$

where $\tilde{T}_j^i$ is the measured temperature at time t_j and abscissa z_i . On the experimental bench, the sensors are placed in the middle of each disk. As the first and the last sensors are used as boundary conditions, the number of sensors used in the procedure is seven ($N = 7$). The time step number is 3600 ($M = 3600$). T_j^i is the calculated temperature at the same time and the same abscissa. The problem is nonlinear concerning the parameters, and we could use a Gauss Newton Method or a trust-region method [33], [34] to identify the parameter vector β. This identification procedure was validated on a numerical case [29], where measurement data were simulated with the 1D numerical model with an assumption of a linear variation for the heat generated flux.

2.5 Sensitivity analysis

A sensitivity analysis on the parameters is conducted to verify their identifiability. The parameters are defined as $\beta_p = \varphi_{ip}^k$ with $p = N_p (k-1) + ip$. We denote the sensitivity matrix of the problem as:

$$X = \left[X_{\beta_1} \; X_{\beta_2} \cdots X_{\beta_p} \cdots X_{\beta_{64}} \right] \tag{3}$$

with the column vector for each parameter β_p,

$$X_{\beta_p} = \begin{bmatrix} X_{\beta_p}^1 \\ \vdots \\ X_{\beta_p}^i \\ \vdots \\ X_{\beta_p}^N \end{bmatrix} \tag{4}$$

The sensitivity vector X_{β_p} is composed of the time sensitivities (index *j*) for each measurement point $X^i_{\beta_p}$:

$$X^{\,i}_{\beta_p} = \left[\frac{\partial T^i_1}{\partial \beta_p} \cdots \frac{\partial T^i_j}{\partial \beta_p} \cdots \frac{\partial T^i_M}{\partial \beta_p} \right]^T \tag{5}$$

All parameters have the same units and can have the same intensity. We will work on dimensionless sensitivities S_{β_p} :

$$S_{\beta_p} = S_{\varphi^k_{ip}} = \frac{X_{\beta_p}}{\max(X)} \tag{6}$$

All the sensitivity vectors are presented in figure 4. The study conditions are similar to those found in the experimental configuration (part 4). In order to illustrate an example of one interface, the figure 5 presents the sensitivity vectors for the parameters φ^4_{ip}. It can be seen that only the sensors on either side of the interface are sensitive to the parameters of this interface.

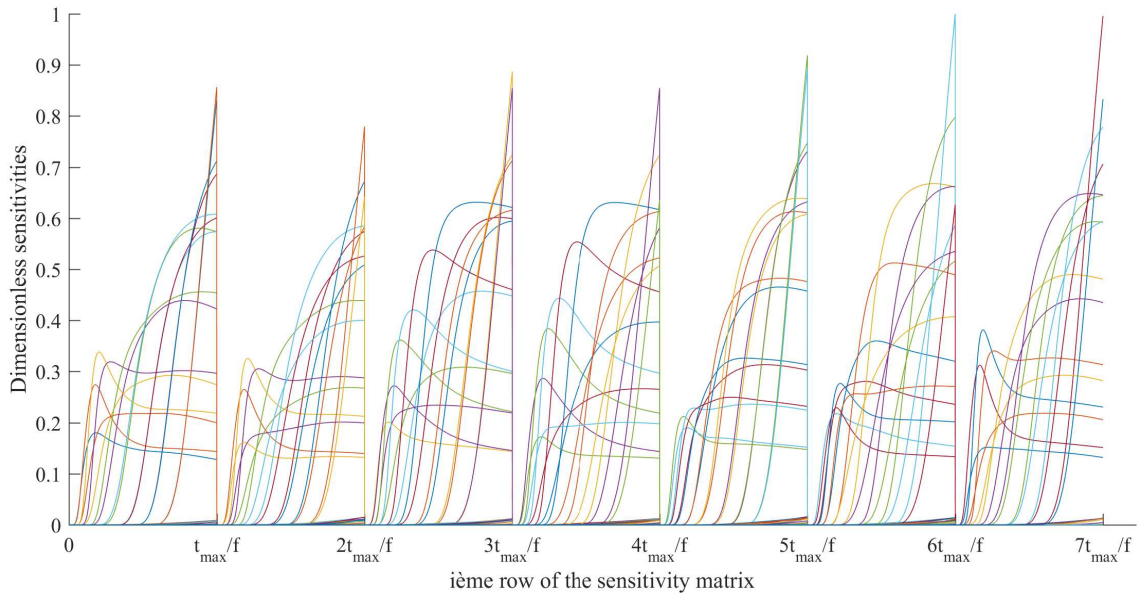

Figure 4. Dimensionless sensitivity vectors of the parameters

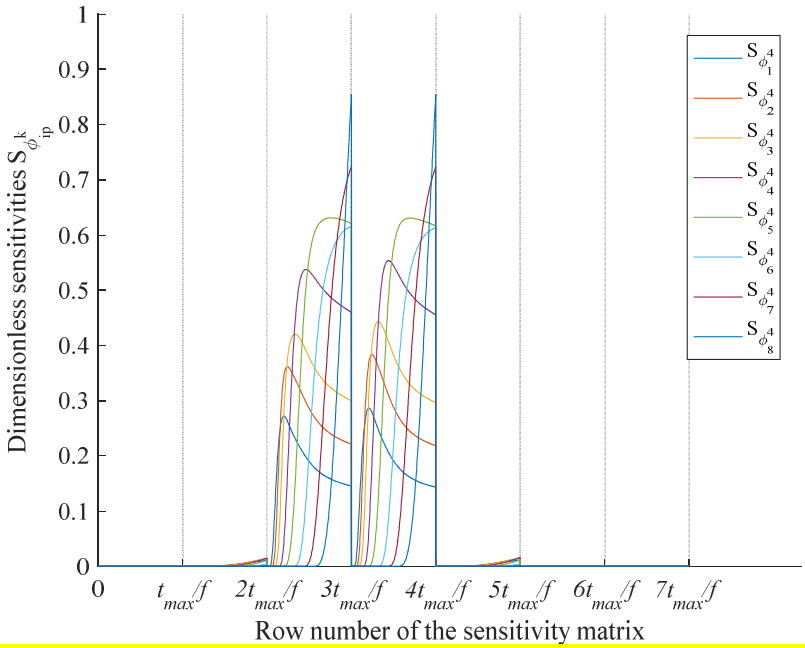

Figure 5. Dimensionless sensitivity vectors of the parameters for the 4t^h interface

The correlation coefficient *cc* between two sensitivity vectors is calculated as

$$cc\left(X_{\beta_p}, X_{\beta_q}\right) = \frac{\left(X_{\beta_p}^T X_{\beta_q}\right)}{\sqrt{\left(X_{\beta_p}^T X_{\beta_p}\right)\left(X_{\beta_q}^T X_{\beta_q}\right)}} \tag{7}$$

The correlations are plotted in figure 6. It can be seen that the correlation only appears between two consecutive parameters at the time of each interface (due to diffusive problem, but less than 90% in our system). It is important to note that the coefficients are widely not correlated between the different interfaces.

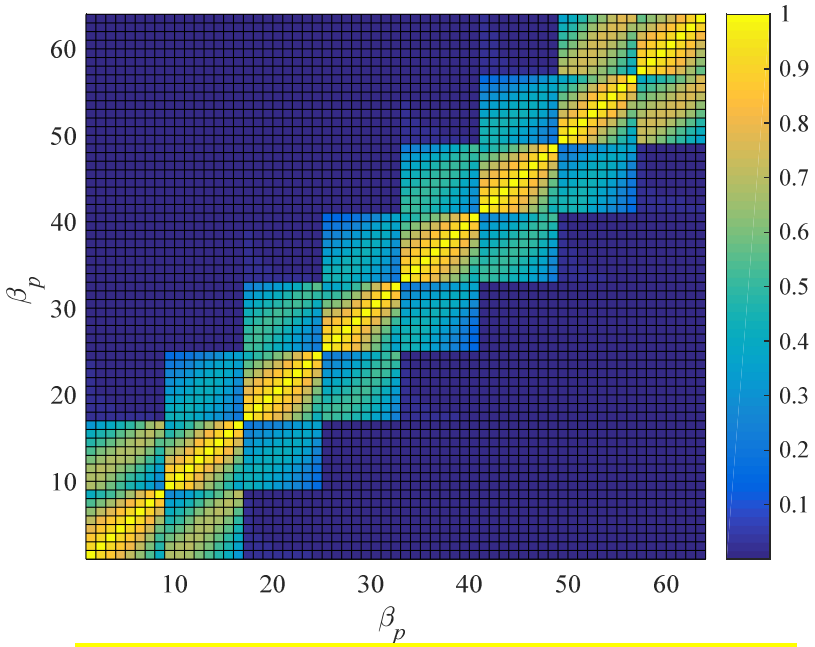

Figure 6. Correlation coefficients between the parameters

3. Experimental Device

3.1. Experimental braking system

Several experimental devices can be used for the wheel and brake equipment tests, including flywheels. The main advantage of flywheels is the capability to reproduce in-landing conditions for the landing gear. The contact between the tire and the track can be reproduced in the way that is shown in figure 7. That is why those machines are preferable for development and qualification tests. The wheel is attached to a frame which is movable in translation. During the trial, the flywheel is rotated at significant speed. The frame translates along the axis, as figure 7 indicates. The wheel is then applied in contact with the flywheel with a defined load.

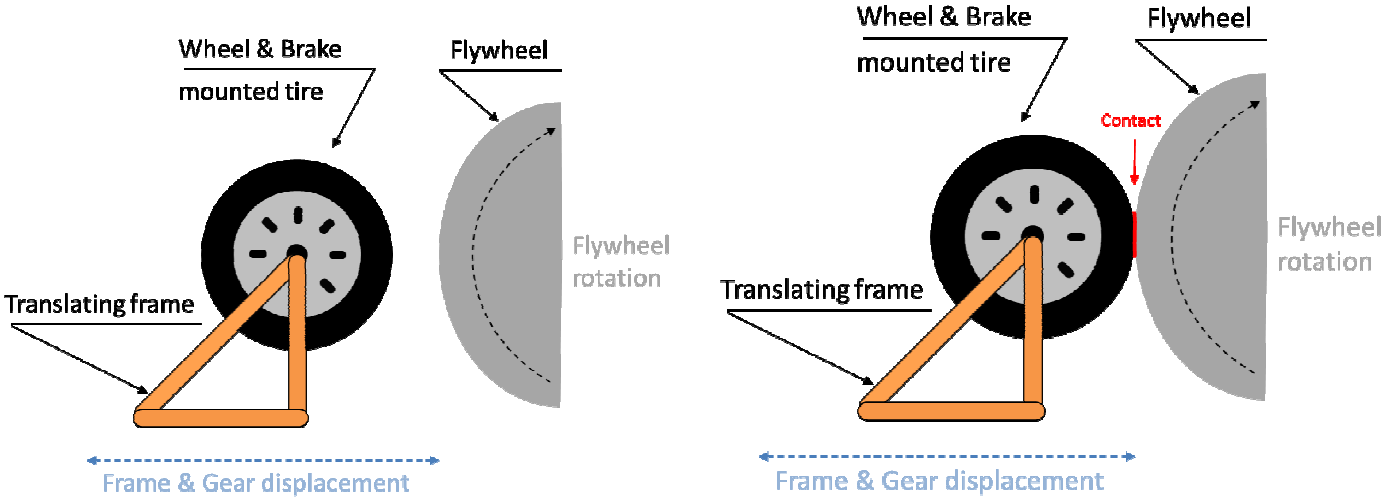

Figure 7. Schematic diagram of the flywheels system

During the braking, the flywheel is let loose from the electric engines used for the rotation setting. The aim of the system is to stop the whole system by preserving its integrity and by ensuring the braking specification such as stopping distance. Two methods can be considered for the test to be a success:

- Brake fluid enslavement, by maintaining the brake fluid at a constant pressure.
- Brake torque enslavement, by maintaining the torque at a constant with pressure fluctuations.

The use of flywheel allows for the reproduction of the plane kinetic energy during the landing. The kinetic energy to absorb E_{CD} must take into account the wheel and brake inertia, as the following formula describes in equation 8.

$$E_{CD} = \frac{\frac{1}{2} \times m_{aircraft} \times V_s^2}{N_{wheels}} + I_{CD} \times \Omega_a^2$$
$$E_{CD} = \frac{1}{2}\left(\frac{m_{aircraft} \times R_a^2}{N_{wheels}} + 2.I_{CD} \right) \times \Omega_a^2 \quad (8)$$
$$E_{CD} = \frac{1}{2} K \Omega_a^2$$

The kinetic energy of the flywheel is $E_v = \frac{1}{2} K_v \Omega_v^2$. The inertia of the flywheel can be identified thanks to the condition $E_v = E_{CD}$. At the contact of the flywheel and the wheel, the linear speeds are the same ($\Omega_a R_a = \Omega_v R_v$) so that:

$$K_v = K \left(\frac{R_v}{R_a} \right)^2 \quad (9)$$

Different cylinders with mass and radius properties can be placed to adjust the total system inertia and reach the desired value of K_v (figure 8).

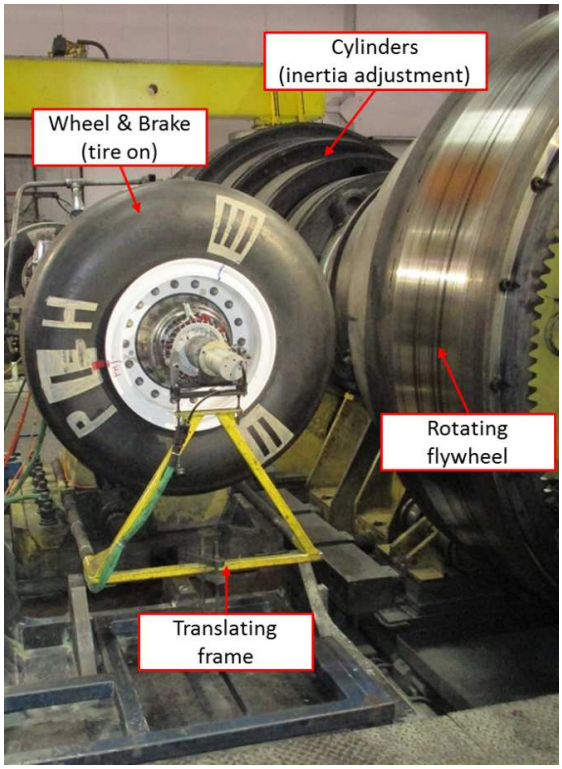

Figure 8. Experimental device

Temperature is measured using type K thermocouples. Some of them are placed on fixed parts of the wheel and brake equipment like stators, the torque tube, the wheel axle or the piston housing. The others are tied to mobile parts of the wheel and brake assembly such as rotors, the wheel or the heat shield. In order to obtain temperature measurements of the mobile parts, the concerned sensors are tied to a rotating collector (figure 9). Other channels on static parts are straightly connected to the acquisition device.

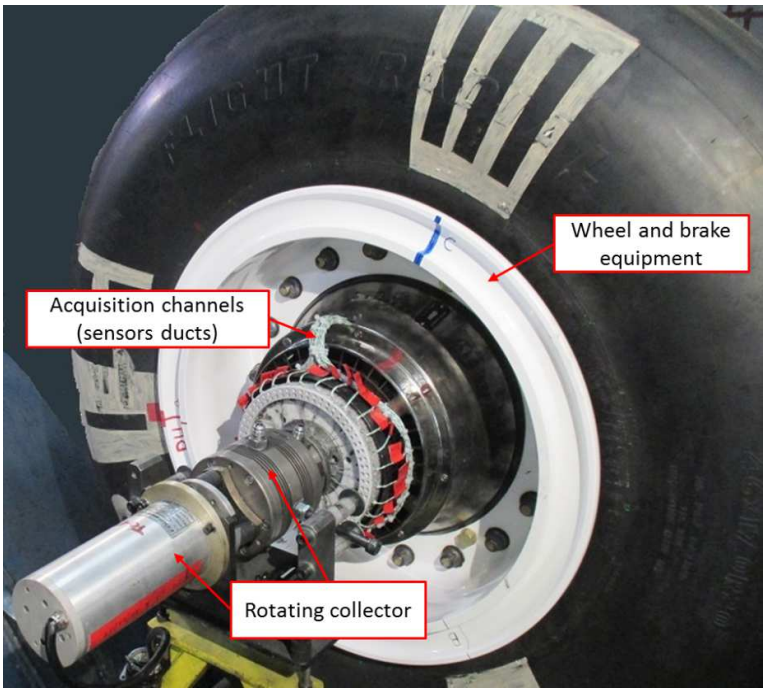

Figure 9. Rotative collector

At the end of the trial, the assembly is dismantled in order to check the integrity of acquisition channels. The purpose of stator and rotor instrumentation is to acquire sufficient information that will lead to successful heat flux identification (figure 10). Temperature is recorded two hundred times per second under braking conditions. The acquisition frequency allows us to track the temperature gradient and evolution during the test with adequate accuracy.

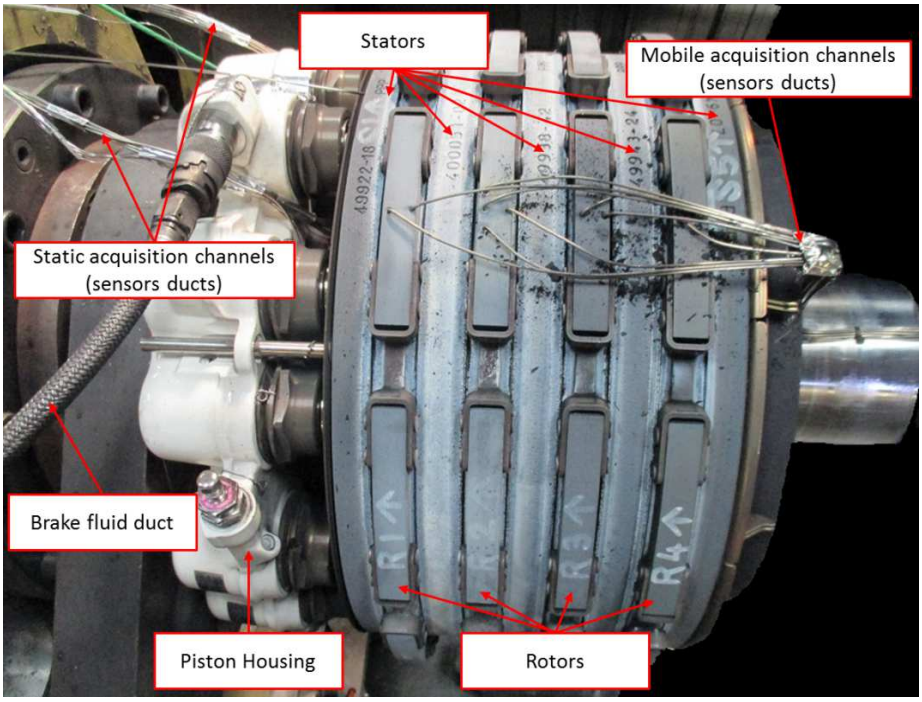

Figure 10. Instrumentation of the brake

3.2. Experimental measurements

The experimental data are presented with the following dimensionless quantities:

$$\varphi_d = \frac{\varphi}{\varphi_{\max}},\ T_d = \frac{T - T_{\min}}{T_{\max} - T_{\min}},\ t_d = \frac{t}{t_{\max}},\ \Delta T = \frac{T_{calculated} - T_{measured}}{T_{\max} - T_{\min}}. \quad (10)$$

Sensors are placed in the middle of each disk. Time evolutions of dimensionless temperatures are presented in figure 11. The use of accurate boundary conditions in the direct problem (convection and radiation) is arduous. Indeed, the convection coefficients are unknown and it is complicated to measure the surface temperatures of the first and last stator.
That is why temperatures of the sensor in the middle of the first and the last stator (S1 and S5) are used as a boundary condition (BC1 and BC2) of the set-up in the numerical model of the inverse method. We use other sensors (R1 to R4) in the minimization procedure in order to identify the generated heat flux.

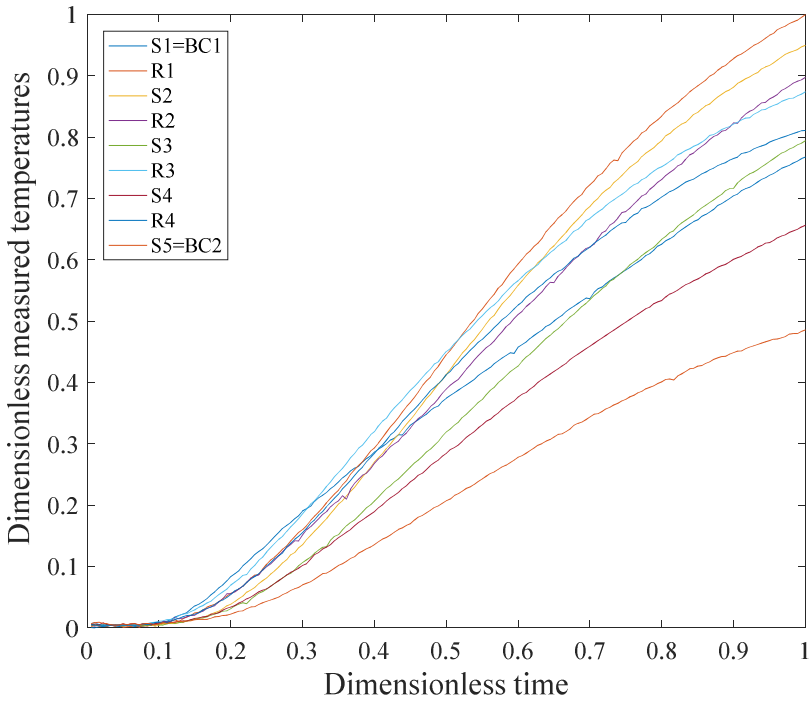

Figure 11. Dimensionless temperature evolution at the center of each disk

4. Results of identification of the generated heat flux

The parameterization described in part 2.3 is used to perform the generated heat flux identification from experimental data. Generated heat flux evolution is linear between two step times. For this identification, the dimensionless time vector chosen is:

$$t_d = [0 \quad 2.8 \quad 5.6 \quad 11.1 \quad 16.7 \quad 27.8 \quad 38.9 \quad 50.0 \quad 66.7 \quad 100 \quad]\% \quad (11)$$

Therefore, the number of unknown parameters to be identified is 64 (8 per interface, with 8 interfaces). For the identification of these parameters, 25200 measurement points will be used in the inversion procedure. It is important to note that estimation procedure results do not

depend on the initialization value of the vector parameter. This predication has been tested and validated.

The different time evolutions of the identified heat generated fluxes are given in figure 12. The comparison between the measured temperatures and the calculated temperatures from theses identified heat generated fluxes for the rotors are presented in figure 13, and in figure 14 for the stators. S1 and S5 are not shown since they are the boundary conditions of the system.

The repartition of the thermal braking energy is shown in figure 15. This result is validated by the thermal residues given in figure 16. They are not signed and their level is very low, since we recognize the measurement noise related to instrumentation and data acquisition. Also, it can be observed that there is a strong disparity in the intensities of the thermal fluxes, and mostly in their temporal evolutions for each interface. We find an increase of the heat generated fluxes in the first-time steps, followed by a decrease during the braking period as illustrated below. This is in line with the expectations from mechanical assumptions.

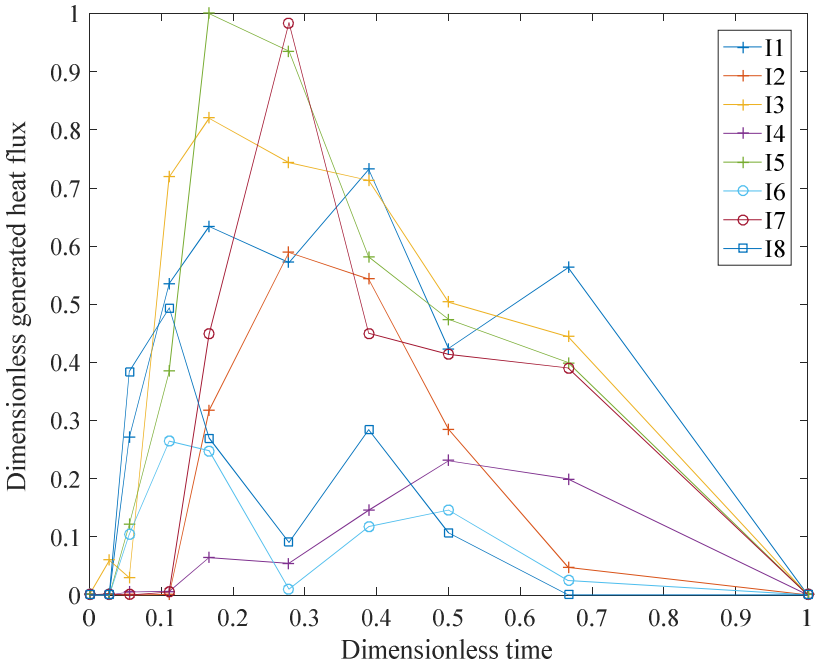

Figure 12. Dimensionless identification of heat generated flux at different interfaces

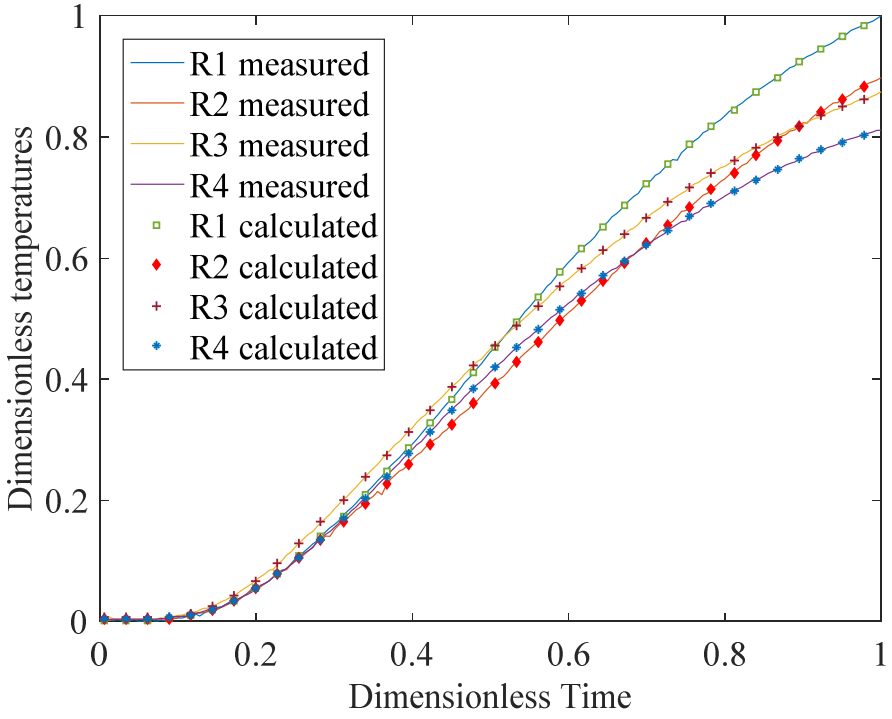

Figure 13. Dimensionless measured temperatures and calculated temperatures from identified heat fluxes in the rotors

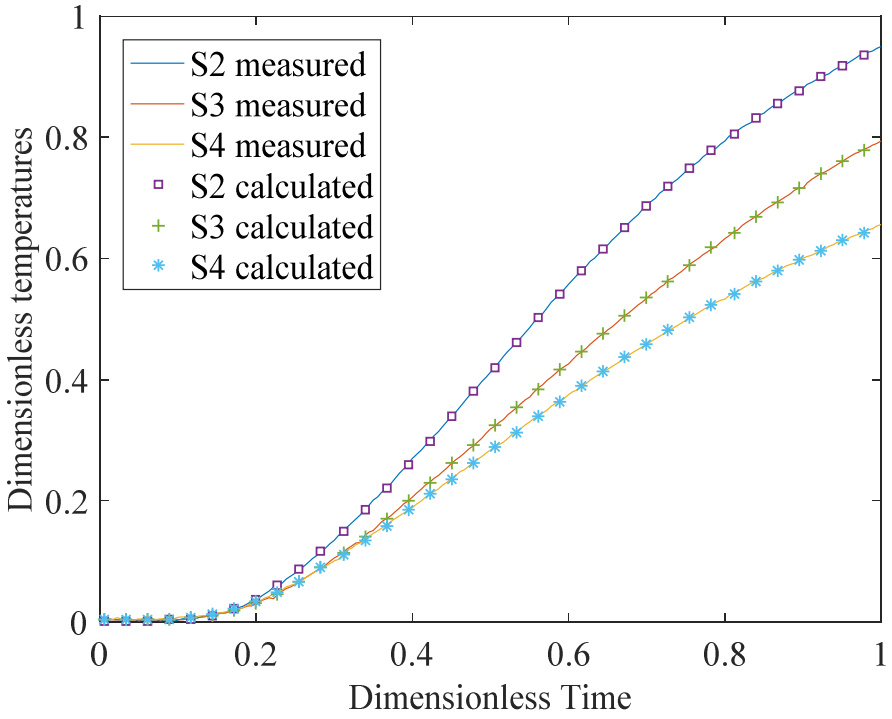

Figure 14. Dimensionless measured temperatures and calculated temperatures from identified heat fluxes in the stators

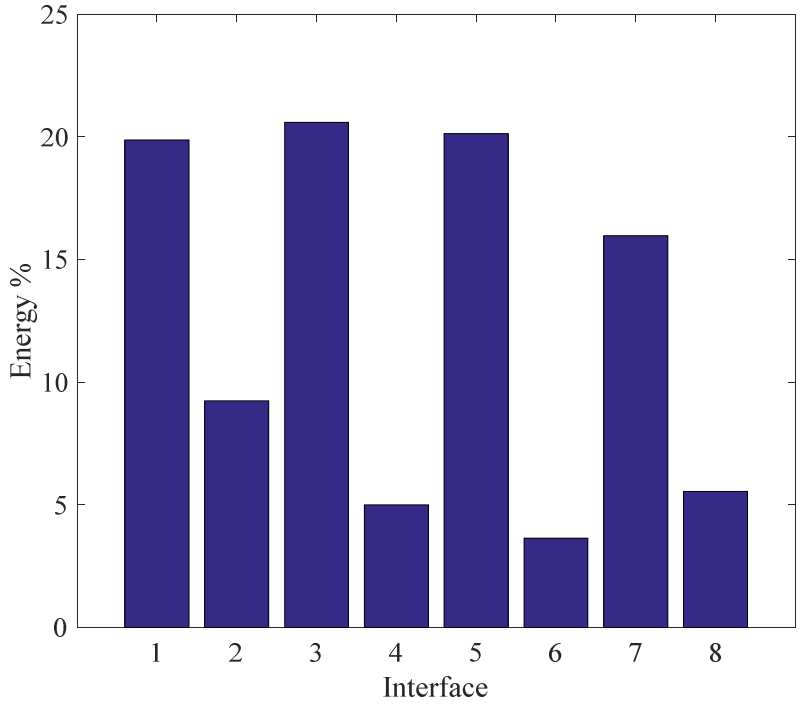

Figure 15. Energy repartition between interfaces

h_L [W.m^{-2}.K^{-1}]	500	10
E_{conv}/E_g [%]	2.79	0.057

Table 1. Percentage of convective energy losses on generated energy for two different values of h_L

ε_L	1	0.1
E_{rad}/E_g [%]	0.97	0.1

Table 2. Percentage of radiative energy losses on generated energy for two different values of ε_L

Table 1 and 2 present the percentages of lateral convective and radiative energy losses of the generated energy, respectively. So the values of the values of the emissivity and the convective coefficient have low effect.

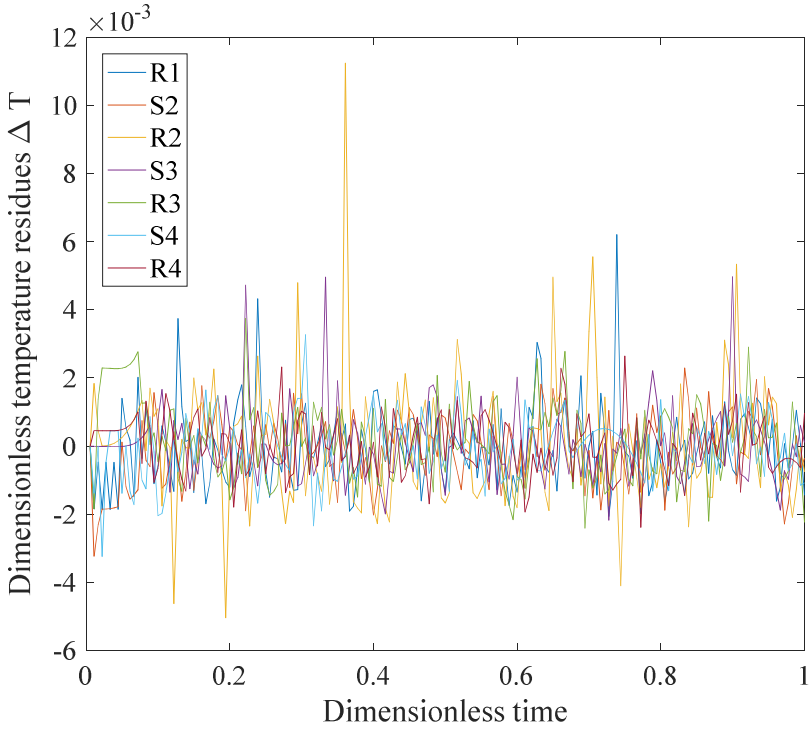

Figure 16. Dimensionless thermal residues for each sensor

Finally, the thermal identified energy is about 9.4% higher than the measured mechanical energy on the test bench. The combination of low unsigned residues with identified heat dissipation energy very close to the one absorbed mechanically and measured during the test confirms the results obtained by identification for the generated heat flux.

5. Conclusion

In this article, we present the estimation of the generated heat flux in aircraft braking system interfaces. The experimental device is described with the thermal instrumentation of the static and rotating part of the brake. Following, an identification procedure is performed from experimental data using the assumption of linear variation over time intervals on the generated heat flux. From this assumption, the identification provides some accurate results: the residues are not signed and are very low, the temporal evolution is physical, and the identified thermal energy is very close to the degraded mechanical energy measured during the test.

This is the first time that a study identifies the real generated heat flux by friction in an aircraft brake system. It is necessary to carry out further tests under similar braking conditions in order to confirm these first results. However, the experimental instrumentation of the brake system coupled to the inverse method provides accurate heat generated fluxes. This could then be used to improve 3D numerical models in order to predict overall temperatures of the braking system during the braking period, as well as during the cooling period which will follow.

Acknowledgements

The authors are grateful for SAFRAN LANDING SYSTEMS for their technical support. This work was supported by the National Association of Research and Technology (ANRT).

Nomenclature

a	Thermal diffusivity	$[m^2.s^{-1}]$
E_{CD}	Kinetic energy to absorb	[J]
E_v	Kinetic energy of the flywheel	[J]
E_{conv}	Lateral energy loss by convection	[J]
E_g	Generated energy by friction	[J]
E_{rad}	Lateral energy loss by radiation	[J]
h	Convection coefficient	$[W.m^{-2}.K^{-1}]$
h_L	Lateral convection coefficient	$[W.m^{-2}.K^{-1}]$
I_{CD}	Brake moment of inertia	$[kg.m^2]$
K	Wheel and brake moment of inertia	$[kg.m^2]$
K_v	Flywheel moment of inertia	$[kg.m^2]$
$m_{aircraft}$	Aircraft mass	[kg]
M	Number of step time measurement	[-]
N	Number of sensors	[-]
Np	Number of parameters for each interface	[-]
N_{wheels}	Number of braking wheels	[-]
R_a	Apparent radius of the tire	[m]
R_{ext}	External radius of the break disc	[m]
R_{int}	Internal radius of the break disc	[m]
R_v	Flywheel radius	[m]
R_{TSC}	Thermal sliding contact resistance	$[m^2.K.W^{-1}]$
S_L	Lateral surface of the disk	$[m^2]$
T_0	Ambient temperature	[K]
T_c	Contact temperature	[K]
T_d	Dimensionless temperature	[-]
T_{min}	Minimum temperature in the system	[K]
T_{max}	Maximum temperature in the system	[K]
T	Calculated temperature in Rotor and Stator	[K]
$\tilde{T}$	Measured temperature in Rotor and Stator	[K]
t	Time	[s]
t_{max}	Time of the maximum generated heat flux	[s]
t_d	Dimensionless time	[-]
V_s	Aircraft speed at braking start	$[m.s^{-1}]$
z	Abscissa	[m]
α	Local heat partition coefficient	[-]
β	Vector of parameters	[-]
$\hat{\beta}$	Estimated vector of parameters	[-]
ΔT	Dimensionless thermal residues	[-]
ε	Discrepancy	[%]
ε_L	Lateral emissivity	[%]
φ_q	Generated heat flux	$[W.m^{-2}]$
φ_d	Dimensionless generated heat flux	[-]
φ_{max}	Maximum of the time evolution of the generated heat flux	$[W.m^{-2}]$
λ	Thermal conductivity	$[W.m^{-1}.^{K-1}]$
Cp	Thermal Capacity	$[J.kg^{-1}.K^{-1}]$
Ω_a	Wheel rotating speed	$[rad.s^{-1}]$
Ω_v	Flywheel rotating speed	$[rad.s^{-1}]$
σ	Stephan Boltzmann constant	$[W.m^{-2}.K^{-4}]$
i	index of the sensor	[-]

ip	index of the parameters for each interface	[-]
j	index of the time step	[-]
k	index of the interface	[-]
l	Left disk	[-]
r	Right disk	[-]
S	Heatshield	[-]
T	Torque Tube (axis)	[-]
1	Left boundary condition	[-]
2	Right boundary condition	[-]

References

[1] M. N. Ozisik, *Inverse Heat Transfer: Fundamentals and Applications*. CRC Press, 2000.

[2] J. V. Beck, B. Blackwell, and C. R. S. C. Jr, *Inverse Heat Conduction: Ill-Posed Problems*. James Beck, 1985.

[3] O. M. Alifanov, *Inverse Heat Transfer Problems*. Springer Science & Business Media, 2012.

[4] J. V. Beck, 'Nonlinear estimation applied to the nonlinear inverse heat conduction problem', *Int. J. Heat Mass Transf.*, vol. 13, no. 4, pp. 703–716, Apr. 1970.

[5] D. Maillet, T. Metzger, and S. Didierjean, 'Integrating the Error in the Independent Variable for Optimal Parameter Estimation Part I: Different Estimation Strategies on Academic Cases', *Inverse Probl. Sci. Eng.*, vol. 11, no. 3, pp. 175–186, Jun. 2003.

[6] D. Maillet and D. Petit, 'Techniques inverses et estimation de paramètres. Partie 1', *Tech. Ing. Phys. Stat. Mathématique*, vol. base documentaire : 42619210., no. ref. article : af4515, 2008.

[7] T. Moussa, B. Garnier, U. Pelay, Y. Favennec, and H. Peerhossaini, 'Heat transfer at the grinding interface between glass plate and sintered diamond wheel', *Int. J. Therm. Sci.*, vol. 107, pp. 89–95, Sep. 2016.

[8] B. Ghadimi, F. Kowsary, and M. Khorami, 'Thermal analysis of locomotive wheel-mounted brake disc', *Appl. Therm. Eng.*, vol. 51, no. 1–2, pp. 948–952, Mar. 2013.

[9] Z. Zhu, Y. Peng, Z. Shi, and G. Chen, 'Three-dimensional transient temperature field of brake shoe during hoist's emergency braking', *Appl. Therm. Eng.*, vol. 29, no. 5–6, pp. 932–937, Apr. 2009.

[10] F. Talati and S. Jalalifar, 'Analysis of heat conduction in a disk brake system', *Heat Mass Transf.*, vol. 45, no. 8, pp. 1047–1059, Jun. 2009.

[11] A. Baïri, N. Alilat, J.-G. Bauzin, and N. Laraqi, 'Three-dimensional stationary thermal behavior of a bearing ball', *Int. J. Therm. Sci.*, vol. 43, no. 6, pp. 561–568, Jun. 2004.

[12] N. Laraqi, 'Températures de contact et coefficient de partage de flux généré par frottement sec entre deux solides. Approche nouvelle de la génération de flux', *Int. J. Heat Mass Transf.*, vol. 35, no. 11, pp. 3131–3139, Nov. 1992.

[13] A. Hocine, N. Alilat, and J.-G. Bauzin, 'Comportement thermique d'un disque tournant soumis à des sources de chaleur surfaciques discrètes', *Comptes Rendus Mécanique*, vol. 337, no. 8, pp. 616–620, Aug. 2009.

[14] N. Laraqi, 'An Exact Explicit Analytical Solution of the Steady-State Temperature in a Half Space Subjected to a Moving Circular Heat Source', *J. Tribol.*, vol. 125, no. 4, pp. 859–862, Sep. 2003.

[15] Y.-C. Yang and W.-L. Chen, 'A nonlinear inverse problem in estimating the heat flux of the disc in a disc brake system', *Appl. Therm. Eng.*, vol. 31, no. 14–15, pp. 2439–2448, Oct. 2011.

[16] B. Ghadimi, F. Kowsary, and M. Khorami, 'Heat flux on-line estimation in a locomotive brake disc using artificial neural networks', *Int. J. Therm. Sci.*, vol. 90, pp. 203–213, Apr. 2015.

[17] M. P. Dyko and B. T. F. Chung, 'Finite element thermal model of an aircraft wheel and carbon brake assembly', *SAE Trans.*, vol. 99, no. 1, pp. 1723–1737, 1990.

[18] Z. Wolejsza, A. Dacko, T. Zawistowski, and J. Osinski, 'Thermo-Mechanical Analysis of Airplane Carbon-Carbon Composite Brakes Using MSC.Marc', in *MSC.Software Corporation's Worldwide Aerospace Conference and Technology Showcase*, Toulouse, France, 2002, vol. Paper 2001-58, p. 12.

[19] Yinghui Song, Yuren Li, and Bo Liang, '3-D transient temperature field analysis for aircraft brake system', 2011, pp. 903–906.
[20] T. Montrol-Amouroux, 'Étude et modélisation thermique simplifiée d'un équipement roue et frein aéronautique en phase de pré-étude', Lyon, INSA, Lyon, 2013.
[21] B. B. Shivakumar, C. Ganga Reddy, and P. Jayasimha, 'Thermal management of aircraft braking system', *Int. J. Sci. Technol. Manag.*, vol. 04, no. Special Issue 01, pp. 143–152, Feb. 2015.
[22] A. N. Tikhonov and V. I. Arsenin, *Solutions of ill-posed problems*. Washington; New York: Winston ; Distributed solely by Halsted Press, 1977.
[23] O. M. Alifanov, E. A. Artiukhin, and S. V. Rumiantsev, *Extreme Methods for Solving Ill-Posed Problems With Applications to Inverse Heat Transfer Problems*. New York: Begell House, 1995.
[24] P. Le Masson, T. Loulou, E. A. Artiukhin, P. Rogeon, D. Carron, and J. J. Quemener, 'A numerical Algorithm for estimating the convection heat transfer coefficient during a metallurgical "Jominy end-quench" test', in *Computational heat and mass transfer – CHMT 2001- Vol.II*, Rio de Janeiro, 2001.
[25] Y. Jarny, 'Inverse Problems - Part A: Regularized Solutions', in *Proceedings of the 5th METTI School*, Roscoff, France, 2011, vol. Lecture 9.
[26] D. Maillet, Y. Jarny, and D. Petit, 'Problèmes inverses en diffusion thermique Modèles diffusifs, mesures, sensibilités', *Tech. Ing. Transf. Therm.*, vol. base documentaire : TIB214DUO., no. ref. article : be8265, 2010.
[27] J.-P. Bardon, 'Bases physiques des conditions de contact thermique imparfait entre milieux en glissement relatif, Revue Générale de Thermique', *Rev. Générale Therm.*, vol. 386, pp. 86–91, 1994.
[28] A. A. Tseng, 'Thermal Modeling of Roll and Strip Interface in Rolling Processes: Part 1-Review', *Numer. Heat Transf. Part Appl.*, vol. 35, no. 2, pp. 115–133, Feb. 1999.
[29] J.-G. Bauzin, N. Keruzore, A. Gapin, J.-F. Diebold, and N. Laraqi, 'Characterization of the thermal contact parameters in an airplane braking system using inverse methods', in *Third international conference on Thermophysical and Mechanical Properties of Advanced Materials, THERMAM 2016*, Izmir, 2016, pp. 219–228.
[30] J.-G. Bauzin and N. Laraqi, 'Méthodologie d'identification des paramètres thermiques d'un contact glissant', presented at the Colloque Inter-universitaire Franco-Québecois, Saint lô, France, 2017, p. Art 08-08.
[31] J.-G. Bauzin and N. Laraqi, 'Simultaneous Estimation of Frictional Heat Flux and Two Thermal Contact Parameters for Sliding Contacts', *Numer. Heat Transf. Part Appl.*, vol. 45, no. 4, pp. 313–328, Mar. 2004.
[32] J.-G. Bauzin, N. Laraqi, and A. Baïri, 'Estimation of thermal contact parameters at the interface of two sliding bodies', *J. Phys. Conf. Ser.*, vol. 135, p. 012015, Nov. 2008.
[33] J. J. Moré and D. C. Sorensen, 'Computing a Trust Region Step', *SIAM J. Sci. Stat. Comput.*, vol. 4, no. 3, pp. 553–572, Sep. 1983.
[34] T. F. Coleman and Y. Li, 'An Interior Trust Region Approach for Nonlinear Minimization Subject to Bounds', *SIAM J. Optim.*, vol. 6, no. 2, pp. 418–445, May 1996.